2012-05

# In Situ Heading Drift Correction for Human Position Tracking Using Foot-Mounted Inertial/Magnetic Sensors

Bachmann, Eric

2012 IEEE International Conference on Robotics and Automation
RiverCentre, Saint Paul, Minnesota, USA
May 14-18, 2012

# In Situ Heading Drift Correction for Human Position Tracking Using Foot-Mounted Inertial/Magnetic Sensors

Eric Bachmann, James Calusdian, Eric Hodgson, and Xiaoping Yun

*Abstract* — **This paper presents a heading drift correction method and experimental results for position tracking of human movement based on the use of foot-mounted inertial/magnetic sensor modules. A position tracking algorithm was previously developed, which incorporated a zero velocity update technique for correcting accelerometer drift. Previous experiments indicated the presence of a persistent heading drift in the estimated position. In this paper, a simple method for correcting this drift is presented. The method requires the user to walk over a closed loop path with the foot-mounted sensor module. Assuming a constant sensor bias for this initial walk, the resulting position error is then used to accomplish an in situ correction for position estimates during future walks. Experimental results validate the effectiveness of the drift correction method and show a significant improvement in position tracking accuracy. Accuracy is determined based on the final position estimates following walks of 100 and 400 meters. Estimated distance traveled averages within 0.2% of actual distance traveled and distance from the actual position averages within 0.28% of actual distance traveled.**

## I. Introduction

In the future, robots will be expected to interact with humans in natural unstructured environments. For this and other applications such as telerobotics and portable immersive virtual reality systems, there is a need to develop techniques for tracking human movement that are self-contained, do not rely on any infrastructure support, and can be deployed in any environment. This paper presents resent experimental results on position tracking of human movement using foot-mounted inertial/magnetic sensor modules.

Miniature sensor modules containing accelerometers, magnetometers, and angular rate sensors are now widely available commercially. These units are low power, light weight, and small enough so that they can be easily attached to one's shoe for use in inertial position tracking applications. One factor that has presented a significant challenge is the presence of random noise in MEMS-based accelerometers and angular rate sensors that are utilized within the sensor modules. One approach to overcome this problem is a technique called zero-velocity updates (ZUPT).Various researchers have documented their work utilizing this approach, for example [1], [2], and [3]. In addition to this, researchers have employed other techniques to increase the overall accuracy. For example, in [4] an initial in situ calibration is accomplished prior to first use wherein the foot-mounted sensor module is rotated with minimum translation to characterize the magnetometers. In [5] a rigorous laboratory characterization of the angular rate sensors is performed to compensate for temperature and acceleration-dependent bias. If the sensor bias is relatively constant, then a "slope-correction" scheme can be used, as in [6].

At present, orientation estimation algorithms for inertial/magnetic sensor modules remain dependent upon magnetometers to determine attitude within the horizontal plane. Due to hard and soft iron interference [7], low-cost magnetometers are unable to precisely measure the components of the Earth's magnetic field vector relative to the sensing unit. In the context of human position tracking, such errors may be caused by metallic items within shoes or clothes as well as distortions of the Earth's magnetic field caused by ferrous objects within the tracking area. These measurement errors will produce inaccurate heading estimates which in turn will result in large position errors even if estimates of distance traveled are extremely accurate.

This paper presents a technique for the correction of heading errors experienced when using foot-mounted inertial/magnetic sensor modules. It is based on making a preliminary in situ measurement of the heading drift, then using this measurement to correct the position estimate during subsequent walks. The paper is organized as follows. Section II describes previous work on our position tracking algorithm, our adaptive-gain complementary filter for the determination of the foot attitude, and a new heading drift correction method. Section III contains the experimental results of our method for heading correction. Finally, Section IV has some concluding remarks and describes future work.

## II. Position Tracking Algorithm

### A. Review of the Original Algorithm

An algorithm for estimating human position during

[1] Manuscript received September 16, 2011. This work was supported in part by the National Science Foundation (NSF) and the Army Research Office (ARO).
Eric R. Bachmann is with the Department of Computer Science and Software Engineering, Miami University, Oxford, OH 45056 USA.
James Calusdian is with the Department of Electrical and Computer Engineering, Naval Postgraduate School, Monterey, CA 93943 USA.
Eric Hodgson is with the Department of Psychology and Armstrong Institute of Interactive Media Studies, Miami University, Oxford, OH 45056 USA.
Xiaoping Yun is with the Department of Electrical and Computer Engineering and MOVES Institute, Naval Postgraduate School, Monterey, CA 93943 USA.

walking and running was initially introduced in [8]. A small, self-contained inertial/magnetic sensor module was attached to a shoe of a user. The sensor module provides measurements of the foot motion and outputs three-axis acceleration, angular rate, and local magnetic field in the sensor coordinate. The algorithm first converts the acceleration measurement from the sensor coordinates to the earth fixed coordinates, and then integrates the acceleration twice to obtain foot position. A key feature of the algorithm is the incorporation of a zero velocity update technique that corrects the drift in the acceleration measurement. The drift correcting technique is based on the fact that foot motion is cyclic and foot velocity is zero during the stance phase of foot motion. During the stance phase of every walking step, the estimated velocity obtained from integrating the foot acceleration measurement is compared with the known velocity of the foot, which is zero during the stance phase. Any difference is considered to be caused by the drift in the foot acceleration measurement. The amount of drift is then estimated based on the velocity difference and the duration of the step, and a correction is applied to the acceleration measurement.

A detailed analysis of the position tracking algorithm was conducted in [9]. As mentioned above, the foot acceleration measurement in the sensor coordinates must be converted into the earth fixed coordinates prior to integration. The conversion requires an estimate of foot orientation. The *dynamic* accuracy of the foot orientation estimation algorithm is an important factor that affects the accuracy of the position tracking algorithm. As a result, an adaptive-gain complementary filter was specially designed for estimating foot orientation. The complementary filter takes into consideration the cyclic nature of foot motion. During the stance phase of foot motion, foot velocity is zero or near zero and complementary filter relies more on accelerometer and magnetometer measurements to estimate foot orientation. During the swing phase, on the other hand, the complementary filter relies more on angular rate measurements to estimate foot orientation. A single filter gain is adaptively adjusted to blend the measurement data in the two phases of foot motion. It has been shown that the adaptive-gain filter out-performs filters with fixed gain in attaining higher dynamic accuracy.

With the adaptive-gain complementary filter, extensive simulation and experimental testing of the position tracking algorithm was carried out in [9]. It was shown that the achievable position accuracy of the algorithm is about 1% of the total walked distance.

### B. *Heading Drift Correction Method*

To assess the accuracy of the position tracking algorithm, two types of walking experiments were conducted. In the first type of experiments, users were instructed to walk along a straight-line path for a fixed distance (e.g., 100 meters). In the second type of experiments, users were directed to begin from a starting position, walk along a circular or oval path of a known distance, and return to the starting position. In the straight line walking experiment, it was observed that the estimated walking paths were fairly straight, but the directions of the paths slightly differed from one sensor module to another. This suggested that there might be a heading drift in sensor measurements and that this heading drift was relatively constant for each sensor. In the circular path experiment, while the users walked a complete loop and returned to the starting position, the end point of the estimated paths did not meet the starting point. Instead, the end point tended to consistently be in a particular area relative to the starting point for each sensor module used in the experiment. The fact that the end points of the estimated circular paths were not randomly distributed and were rather clustered in a region relative to the starting point also suggested a heading drift in sensor measurements.

The systematic nature of the observed errors suggested a *zero position update* that is similar in approach to the zero velocity updates that are applied at the completion of each swing phase. A method for correcting heading drift is developed and is described below. A user is instructed to walk along a circular path and return to the initial starting point. The trajectory of the walked path is computed using the position tracking algorithm. Ideally, the computed end point should coincide with the starting point, forming a closed path. As discussed above, however, the computed end point is typically different from the starting point. A difference vector is computed:

$$\Delta p = p_{init} - p_{end} \tag{1}$$

where $p_{init}$ and $p_{end}$ are 3-dimesional position vectors of the initial starting point and the end point. Based on this difference vector, a drift correction vector is then computed:

$$\Delta v = \frac{\Delta p}{T_{total}} \tag{2}$$

where $T_{total}$ is the total cumulative integration time of the circular path. It is noted that integration happens only during the swing phase. A drift correction vector is thus created for a specific sensor module.

In the subsequent use of the sensor module for which a drift correction vector was established, a correction is applied to the estimated position as follows. At the end of each swing phase, a correction is applied to the estimated position using the drift correction vector:

$$p_c = p_e + \Delta v * T_{swing} \tag{3}$$

where $p_e$ is the estimated position from the position tracking algorithm, $T_{swing}$ is the total time period of the latest swing phase that was just completed, and $p_c$ is the corrected position.

## III. Experimental Results

The effectiveness of the heading drift correction method was evaluated through a series of experimental trials involving four different human participants walking on an outdoor running track. All subjects were male, ranging in age between 25 and 55. In each trial, the participant was required to make a circuit around the 400 meter track and then perform one or more 100 meter straight line walks in either a northern or southern direction. In one case, the participant completed several additional 400 meter walks around the track. In the trials, the first 400 meter circuit walk was used to obtain a correction vector. The vector was then used to correct heading drift in the 100 meter walks and any subsequent 400 meter walks performed by the participant.

During each the trial, the participant wore a MicroStrain 3DM-GX3-25 inertial/magnetic sensor module on each foot. The sensor modules were encased in foam rubber sleeves to provide shock protection and attached to the feet using two Velcro straps (Figure 1). The sensors were powered by and connected via a USB interface to a Dell Precision M4500 laptop computer with an Intel Core i7 CPU and 8.0 GB of RAM. The laptop was carried by the participant while walking. All data processing and position estimates were produced using software running on the laptop. During several of the trials, the laptop was simultaneously running an immersive virtual reality application which required rendering a virtual world at a resolution of 1280 x 1024 and simultaneously processing data from additional, unrelated hardware. This additional processing load had no effect on position estimate accuracy. The sampling rate for all trails was controlled to a value of approximately 165 Hz. Parameters within the position tracking algorithm were dynamically adjusted at run time to account for any fluctuations in sampling rate.

Walks of 400 and 100 meters were conducted as follows. Prior to each 400 meter walk a mark on the track was designated as the starting and stopping point. Participants were instructed be as accurate as possible in starting and stopping on the mark. In addition, they were instructed to walk the with one foot staying as much as possible on the inner most line of the track in order to produce data that corresponded to a walk of 400 meters. Each 100 meter walk

Fig. 1. MicroStrain 3DM-GX3-25 inertial/magnetic sensor module attached to the feet for position tracking

in a straight line was also performed on the track while walking on one of the 100 meter straight-a-ways using marks placed for track and field events as starting and stopping points.

### A. Uncorrected Results

For the purpose of providing a baseline, Table 1 provides uncorrected results for each of the 100 meter walks and Table 2 provides uncorrected results for each of the 400 meter walks. The results displayed focus on the accuracy of estimated position and estimated distance traveled at the end of each walk. All distances are expressed in meters. Each table includes individual results for each sensor as well as results which combine the estimates of both sensors. This combined estimate is calculated by the system in real-time and would be appropriate for use in immersive virtual reality or tele-robotic applications. *Distance from Start* expresses the vector difference between the starting and ending positions. For perfectly measured 100 meter walks, this figure should be 100 meters. For 400 meter walks, which start and end at the same position, it should be zero. *Elapsed Distance* is the sum of the lengths of all strides that occurred during the walk. For perfectly measured 100 meter walks, the elapsed distance should be 100 meters. For 400 meter

TABLE 1
SUMMARY OF RESULTS FOR UNCORRECTED 100 METER WALKS

| | | Sensor 1 Estimates | | Sensor 2 Estimates | | Combined Sensor Estimates | |
|---|---|---|---|---|---|---|---|
| Subject | Trial | Distance. From Start | Elapsed Distance | Distance. From Start | Elapsed Distance | Distance From Start | Elapsed Distance |
| 1 | 1 | 101.39 | 101.71 | 99.31 | 99.34 | 100.20 | 100.52 |
| 1 | 2 | 99.86 | 100.22 | 100.25 | 100.27 | 100.00 | 100.24 |
| 1 | 3 | 100.87 | 101.03 | 99.44 | 99.59 | 99.54 | 100.31 |
| 1 | 4 | 100.67 | 100.89 | 100.03 | 100.09 | 100.00 | 100.49 |
| 2 | 5 | 99.97 | 100.02 | 98.53 | 98.78 | 99.09 | 99.40 |
| 3 | 6 | 101.23 | 101.54 | 101.43 | 101.48 | 101.43 | 101.51 |
| 4 | 7 | 97.83 | 97.90 | 97.72 | 97.94 | 96.68 | 97.92 |
| Average | | 100.26 | 100.47 | 99.53 | 99.64 | 99.56 | 100.06 |
| % Error | | 0.26 | 0.47 | 0.47 | 0.36 | 0.44 | 0.06 |

TABLE 2
SUMMARY OF RESULTS FOR UNCORRECTED 400 METER WALKS

| | | **Sensor 1 Estimates** | | **Sensor 2 Estimates** | | **Combined Sensor Estimates** | |
|---|---|---|---|---|---|---|---|
| **Subject** | **Trial** | Distance. From Start | Elapsed Distance | Distance. From Start | Elapsed Distance | Distance. From Start | Elapsed Distance |
| 1 | 1 | 16.00 | 403.87 | 13.97 | 398.27 | 13.63 | 401.07 |
| 1 | 2 | 14.41 | 402.52 | 17.98 | 399.19 | 12.64 | 400.85 |
| 1 | 3 | 14.47 | 402.25 | 16.65 | 399.62 | 11.35 | 400.93 |
| 1 | 4 | 16.51 | 403.23 | 16.77 | 400.75 | 12.95 | 401.99 |
| Average | | 15.35 | 402.97 | 16.34 | 399.46 | 12.64 | 401.21 |
| % Error | | 3.84 | 0.74 | 4.09 | 0.14 | 3.16 | 0.30 |

walks, it should be 400 meters. All percentages are determined relative to the total distance traveled.

Figure 2 is a typical position plot for an uncorrected 400 meter walk. It displays individual position plots for each of the foot-mounted sensors as well as a combined position estimate based on averaging the estimates produced for each of the sensor modules. The data in the row labeled as *trial 1* in Table 2 corresponds to the walk shown in Figure 2. For this trial, the error in the average elapsed distance estimate was 1.07 meters or 0.268%. The position error relative to the starting point for *trial one* averaged 13.63 meters or 3.4% of the total distance traveled. In viewing Figure 2, it can be observed that each sensor exhibits unique error characteristics which cause the position estimates to systematically drift in a particular direction. By the end of the walk, the estimated positions have diverged significantly. Since the elapsed distance estimates are highly accurate, it appears that the majority of the error in position estimates is due to errors in azimuth (heading) estimation.

Figure 3 depicts typical results for an uncorrected 100 meter walk. It displays the same kind of systematic drift seen in the 400 meter walk. In Table 1, the row labeled *trial 6* provides quantitative results for the walk shown in Figure 3.

## B. Correction Algorithm Verification

In an initial test of the correction method, a correction vector was determined for data depicted in Figure 2. This correction vector was then reapplied to the data during post-processing. Position errors relative to the starting point for both sensors were reduced to zero (6.63e-006 and 7.35e-006 meters). The corrected plot is depicted in Figure 4. Again, individual position plots for each of the foot mounted sensors as well as the average positions are displayed. While this is a post-processed result, as mentioned above, it does indicate the benefit of the drift correction method.

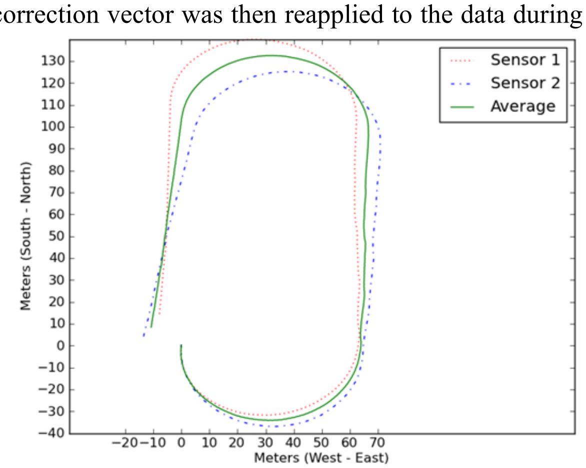


Fig. 2. Uncorrected 400 meter walk

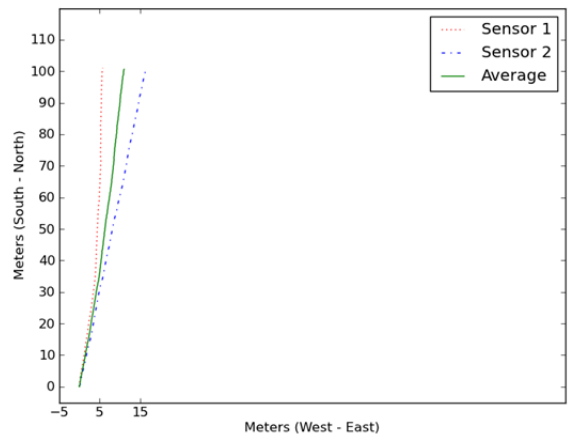


Fig 3. Uncorrected 100 meter walk

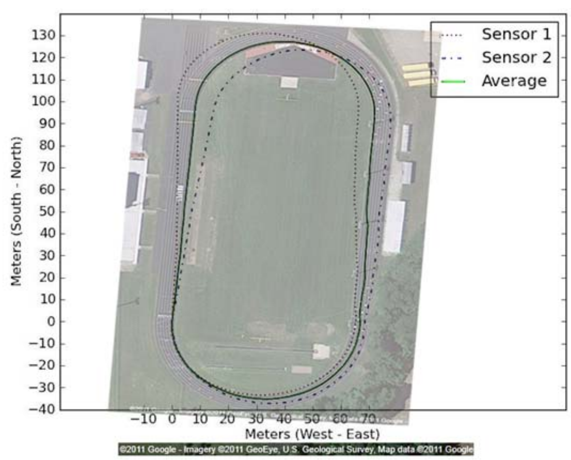


Fig. 4. Post processed 400 meter walk data after application of a correction vector that was derived for the same walk. (Same walk depicted in Figure 2.) Walked path is overlaid on a satellite image of the running track used for data collection. Satellite imagery (c) 2011 GeoEye, U.S. Geological Survey. Map data (c) 2011 Google

### C. *Corrected 100 Meter Walks*

To test the correction method for real-time application, several participants completed a single 400 meter walk in order to produce a correction vector. This vector was then saved and used to correct one or more subsequent 100 meter walks.

Figure 5 depicts the results of applying the correction to the walk depicted in Figure 3. In comparing the two figures, it can be observed that much of the systematic drift was eliminated by the correction and the difference between the position estimates provided by each of the foot mounted sensors is greatly reduced. Table 4 summarizes the corrected results for the same 100 meter walks that are shown in Table 1. In comparing the two tables it can be seen that improvements between Figure 3 and 5 are typical. In all cases the systematic drift was significantly reduced resulting in qualitative improvement of system performance.

### D. *Corrected 400 Meter Walks*

In a final test of the correction method, a single 400 meter walk was used to produce a correction vector that was used on subsequent 400 meter walks. Figure 6 depicts the results of applying the correction to the walk that is depicted in Figures 2 and 4. Table 4 summarizes the corrected results for the same walks that are summarized in Table 2. A comparison of the tables indicates that correction at least halved the magnitude of all errors. Of particular note is the accuracy of the estimates produced by combining the data for both sensors. On average, the estimated distance between the start and end points is within 0.28 % of the distance traveled. On average, the estimated elapsed distance is within 0.20% of the distance traveled. Figure 6 like Figure 5 presents a substantial qualitative improvement in system performance. While the individual sensor position estimates still diverge somewhat from the actual end point for the walk, the divergence is less than half that of the uncorrected results depicted in Figure 2. The average position estimate at the end of the walk appears to be nearly exactly on top of the starting point. The true difference between the start and estimated end point was 0.64 meters or 0.16%.

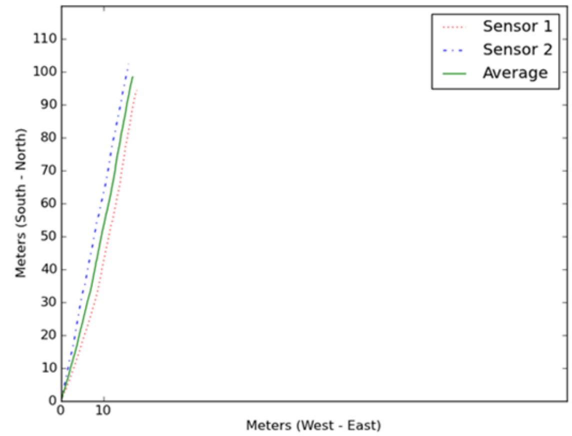


Fig. 5. 100 meter walk results following correction (same walk depicted in Figure 3)

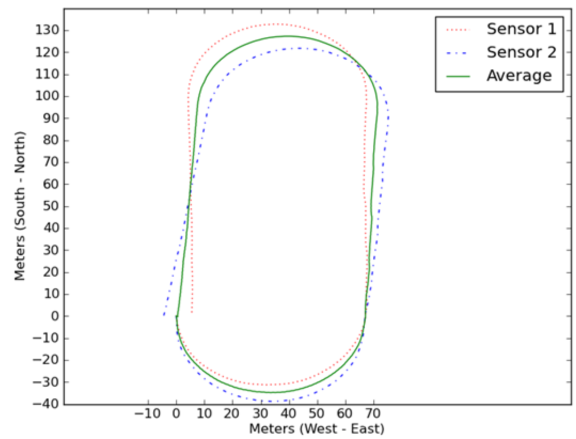


Fig. 6. Corrected 400 meter walk (Same walk depicted in Figure 2.

## IV. Discussion

It is clear that the correction method described here significantly reduces drift and improves the accuracy of position estimates. The applicability of the correction vector obtained for a particular user, particular sensor and environment to another person, sensor, and/or environment

TABLE 3
SUMMARY OF RESULTS FOR CORRECTED 100 METER WALKS

| | | **Sensor 1 Estimates** | | **Sensor 2 Estimates** | | **Combined Sensor Estimates** | |
|---|---|---|---|---|---|---|---|
| **Subject** | **Trial** | Distance. From Start | Elapsed Distance | Distance. From Start | Elapsed Distance | Distance. From Start | Elapsed Distance |
| 1 | 1 | 104.74 | 105.03 | 99.44 | 99.47 | 101.97 | 102.25 |
| 1 | 2 | 96.37 | 96.80 | 99.90 | 99.95 | 98.06 | 98.38 |
| 1 | 3 | 104.36 | 104.51 | 99.45 | 99.60 | 101.36 | 102.05 |
| 1 | 4 | 104.37 | 104.56 | 100.13 | 100.19 | 101.96 | 102.37 |
| 2 | 5 | 93.36 | 93.41 | 101.53 | 101.76 | 97.44 | 97.58 |
| 3 | 6 | 95.98 | 96.48 | 103.55 | 103.60 | 99.75 | 100.04 |
| 4 | 7 | 98.91 | 98.96 | 97.66 | 97.88 | 97.73 | 98.42 |
| Average | | 99.73 | 99.96 | 100.24 | 100.35 | 99.75 | 100.16 |
| % Error | | 0.27 | 0.04 | 0.24 | 0.35 | 0.25 | 0.16 |

TABLE 4
SUMMARY OF RESULTS FOR CORRECTED 400 METER WALKS

| | | Sensor 1 Estimates | | Sensor 2 Estimates | | Combined Sensor Estimates | |
|---|---|---|---|---|---|---|---|
| **Subject** | **Trial** | Distance. From Start | Elapsed Distance | Distance. From Start | Elapsed Distance | Distance. From Start | Elapsed Distance |
| 1 | 1 | 5.86 | 403.56 | 4.95 | 397.81 | 0.64 | 400.69 |
| 1 | 2 | 5.71 | 402.22 | 4.82 | 398.73 | 0.63 | 400.48 |
| 1 | 3 | 7.19 | 401.78 | 4.12 | 399.23 | 1.87 | 400.51 |
| 1 | 4 | 6.20 | 402.79 | 3.41 | 400.30 | 1.40 | 401.54 |
| Average | | 6.24 | 402.59 | 4.32 | 399.02 | 1.14 | 400.80 |
| % Error | | 1.56 | 0.65 | 1.08 | 0.25 | 0.28 | 0.20 |

is unknown. In addition, while 400 meter walks around a running track were used in the results described here it is unknown whether or not a shorter walk or a walks consisting of several smaller circles on top of each other could be as effective or possibly even more effective. Though not displayed in this paper, the magnitudes of the estimation errors for the vertical axis were similar to those seen in the horizontal plane. These results indicate that correction method will allow accurate tracking of vertical movements produced by actions such as walking up stairs or walking over uneven terrain. These questions will be the subject of future research.

## ACKNOWLEDGMENT

The authors would like to thank Robert McGhee for his support and advice.

## V. REFERENCES

[1] K. Sagawa, Y. Satoh, and H. Inooka, "Non-restricted measurement of walking distance," *Proc. of IEEE Int. Conf. on Systems, Man, and Cybernetics*, vol. 3, pp. 1847 - 1852, October 2000.

[2] A. M. Sabatini, C. Martelloni, and S. Scapellato, "Assessment of walking from foot inertial sensing," *IEEE Trans. Biomed. Eng.*, vol. 52, no. 3, pp. 486 - 494, March 2005.

[3] J. Bird and D. Arden, "Indoor navigation with foot-mounted strapdown inertial navigation and magnetic sensors [emerging opportunities for localization]," *Wireless Comm. IEEE*, vol. 18, no. 2, pp. 28 - 35, 2011.

[4] E. Foxlin, "Pedestrian tracking with shoe-mounted inertial sensors," *IEEE Comput. Graph. Appl.*, vol. 25, no. 6, pp. 38 - 46, 2005.

[5] L. Ojeda and J. Borenstein, "Non-GPS navigation with the personal dead-reckoning system," in *SPIE Defense and Security, Unmanned Systems Technology IX*, Orlando, FL, Sept. 2007, pp. 1 - 11.

[6] O. Bebek et al., "Personal navigation via high-resolution gait-corrected inertial measurement units," *IEEE Trans. Instrum. Meas.*, vol. 59, no. 11, pp. 3018 - 3027, Nov. 2010.

[7] E. R. Bachmann, X. Yun, A. Brumfield, “An Investigation of the Effects of Magnetic Variations on Inertial/Magnetic Orientation Sensors,” *IEEE Robotics and Automation Magazine,* Vol. 14, No. 3,September 2007, pp 76-87.

[8] X. Yun, E. R. Bachmann, H. Moore, and J. Calusdian, "Self-contained position tracking of human movement using small inertial/magnetic sensor modules," in *Robotics and Automation, 2007 IEEE Int. Conf.*, Rome, Italy, April 2007, pp. 2526 - 2533.

[9] J. Calusdian, "A personal navigation system based on inertial and magnetic field measurements," Naval Postgraduate School, Monterey, CA, Ph.D. dissertation Spetember 2010.